Quantum Criticality inside the Anomalous Metallic State of a Disordered Superconducting Thin Film

K. Ienaga,* T. Hayashi, Y. Tamoto, S. Kaneko, and S. Okuma†
Department of Physics, Tokyo Institute of Technology, 2-12-1 Ohokayama, Meguro-ku, Tokyo 152-8551, Japan

(Received 27 July 2020; accepted 10 November 2020; published 14 December 2020)

The field-induced superconductor-insulator transition (SIT) in two-dimensional (2D) systems is a famous example of a quantum phase transition. However, an emergence of an anomalous metallic state induced by field has been a long-standing problem in 2D superconductors. While theories predicted that the emergence is attributed to strong phase fluctuations of the superconducting order parameter due to quantum fluctuations, usual resistance measurements have not probed them directly. Here, using Nernst effect measurements, we uncover superconducting fluctuations in the vicinity of the field-induced metallic state in an amorphous Mo_xGe_{1-x} thin film. The field range where the vortex Nernst signals are detectable remains nonzero toward zero temperature, and it locates inside the metallic state defined by the magnetoresistance, indicating that the metallic state results from quantum vortex liquid (QVL) with phase fluctuations due to quantum fluctuations. Slow decay of transport entropy of vortices in the QVL with decreasing temperature suggests that the metallic state originates from broadening of a quantum critical point in SIT.

DOI: 10.1103/PhysRevLett.125.257001

Quantum phase transition (QPT) is a general concept which describes destruction of a long-range order by a nonthermal parameter [1–3]. In the vicinity of the quantum critical point (QCP), strong quantum fluctuations of the order parameter often lead to peculiar states. A famous example of QPT is the field-induced superconductor-insulator transition (SIT) in two-dimensional (2D) superconductors. This transition results from the quantum mechanical requirement that, in a 2D system, both fermion and boson should be localized at zero temperature by defect scattering or repulsive interaction, and otherwise, condense. In the insulating regime near SIT, an unusual insulating state with localized Cooper pairs was theoretically predicted [4,5] and has been indicated by various experiments [6–12].

However, the emergence of the anomalous metallic state between the superconducting phase and the insulating phase makes the problem more difficult to understand [13]. The metallic state is often observed in amorphous films [14–16], Josephson junction arrays [17], and highly crystalline 2D superconductors [18–21] and shows features reminiscent of superconductivity: a saturated resistance much smaller than a normal resistance and a giant positive magnetoresistance (MR). Although theories predicted that the resistive dissipation at zero temperature is attributed to motion of bosonic particles (Cooper pairs and/or vortices) due to quantum fluctuations [22–25], it has not been completely revealed from resistance measurements whether the mobile bosonic particles are really relevant in the metallic state. Furthermore, it still remains unclear why the QPT picture of SIT is modified. One plausible explanation is that finite coupling between a bosonic system and a fermionic background broadens the quantum critical regime near zero temperature [26]. Thus, it is challenging to uncover development of quantum fluctuations of a superconducting order parameter (SOP) across the field-driven superconductor-metal-insulator transition (SMIT).

In this Letter, using the Nernst effect measurement for an amorphous (a-) Mo_xGe_{1-x} thin film, we reveal a quantum criticality inside the metallic state. Main sources of Nernst signals in a superconductor are quasiparticles, mobile vortices (phase fluctuations of SOP) [27–35], and short-lived Cooper pairs in a normal state (amplitude fluctuations) [34–37]. In a single band model, the contribution of quasiparticles is less effective due to Sondheimer cancellation [30]. Furthermore, in an amorphous sample, it is negligibly small because of an extremely short mean free path of the quasiparticles, which is the order of the interatomic distance [11,34,35]. For the amplitude and the phase fluctuations, a Nernst signal N is approximated by $N = R_{\square}\alpha_{xy}$ due to the particle-hole symmetry [36], where $R_{\square}$ is a sheet resistance, and α_{xy} an off-diagonal Peltier coefficient. $R_{\square}$ is zero in the superconducting phase, while α_{xy} vanishes deep inside the insulating phase. Thus, the Nernst effect measurement is a sensitive probe in the fluctuation regime. Quite recently, the first experiment of the Nernst effect through the disorder-driven SIT was reported in an a-InO_x film down to 0.35 K [11]. In that work, a large Nernst signal was observed on the insulating side as well as on the superconducting side, indicating

formation of the localized Cooper pairs in the insulator phase due to quantum fluctuations. The critical exponent of the SIT was also derived by the scaling analysis of α_{xy}. In the present Letter, we perform a comprehensive study of the fluctuations of SOPs throughout the field-driven SMIT by distinguishing between the amplitude and the phase fluctuations, and define different phases in the B-T plane.

An a-Mo_xGe_{1-x} has a weak and randomly distributed pinning potential due to pointlike pinning sites. Moreover, an edge barrier for vortices to enter a sample is less effective in a film sample than in a bulk crystal [38]. An a-Mo_xGe_{1-x} film with a thickness $t = 12$ nm and $x = 0.78$ was prepared by rf sputtering onto a glass substrate with a thickness of 0.15 mm. To obtain a homogeneous film, the substrate was rotated with 240 rpm and kept at room temperature by water cooling during sputtering. The sample surface was covered by SiO after depositing Ag electrodes.

MR and Nernst signals were measured with a similar apparatus to that in Ref. [39] but installed in a dilution refrigerator. The longitudinal voltage V_x and the transverse voltage V_y were measured by a nanovoltmeter with Ag electrodes spaced by 4.2 mm ($= L$) and 5.6 mm ($= l$), respectively. RuO_2 thermometers for measuring a temperature difference $\Delta T = T_{\rm high} - T_{\rm low}$ were thermally connected to Ag electrodes for V_x via Cu wires. The magnetic field was applied perpendicular to the film plane. MR was obtained using standard four-terminal dc and low-frequency ac locking methods (19 Hz) with a bias current of ≥ 30 nA within the Ohmic regime. Nernst signals were obtained from $N = E_y/\nabla T_x = (V_y/l)/(\Delta T/L)$, where the sample temperatures are defined by $T_{\rm ave} = (T_{\rm high} + T_{\rm low})/2$. During field sweep, ΔT's were fixed to be 30%, ~20%, and ~10% of $T_{\rm ave}$ at 0.1 K, 0.2–0.6 K, and 0.8–2.0 K, respectively, to obtain measurable Nernst voltage keeping ΔT as low as possible. For $T_{\rm ave} \geq 0.8$ K, background thermoelectric voltage generated at $\Delta T = 0$ is subtracted from V_y at $\Delta T \neq 0$ at each measurement step by switching off a heater. For $T_{\rm ave} \leq 0.6$ K, ΔT ($\neq 0$) is continuously applied during field sweep. Background voltage is evaluated from V_y in high- and low-field regimes where observable Nernst signals completely vanish. To obtain reliable Nernst signals, we checked reproducibility at least twice at each temperature, and extracted antisymmetric contributions with respect to magnetic field reversal.

A resistance curve at $B = 0$ is shown in Fig. 1(a) as a black line. The critical temperature $T_c = 2.13$ K and the mean field transition temperature $T_{c0} = 2.58$ K are evaluated from the resistance drop below the measurement limit and the midpoint resistance, respectively. T_c is suppressed compared with ~6 K of a thick sample ($t = 300$ nm) [38]. The difference between T_c and T_{c0} reflects the two dimensionality of our film. This is also supported by $t \lesssim \xi(0)$, where the Ginzburg-Landau coherence length $\xi(0) \sim 19$ nm is roughly estimated from the crossover field

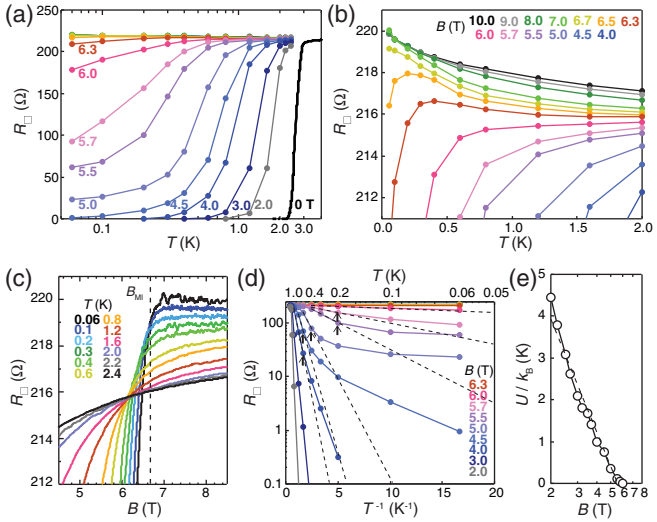

FIG. 1. Field-induced SMIT detected by resistance measurements. (a) Temperature dependence of $R_\square$ at fixed fields. The curves at $B \neq 0$ are converted from MR curves shown in (c). (b) The high-field region of (a) is enlarged. (c) An enlarged view of MR curves obtained at fixed temperatures, exhibiting a crossing behavior around $B_{\rm MI}$ indicated by a dashed line. (d) Arrhenius plots of $R_\square$ at fixed fields. Dashed lines are drawn by a thermal activation formula. Arrows indicate temperatures $T_{\rm cross}$ at which $R_\square$ starts to deviate from the thermal activation formula. (e) Field dependence of U obtained from thermal activation fitting.

$B_{c2}(0) \sim 6$ T, as shown below, and the quantized magnetic flux Φ_0 using $B_{c2}(0) \sim \Phi_0/\xi(0)^2$.

Figures 1(a) and 1(b) display a series of isomagnetic curves exhibiting the field-induced SMIT, which is converted from MR shown in Fig. 1(c). With an increasing field, the isomagnetic curves in the low-temperature region are lifted from zero resistance and show a saturating behavior to nonzero resistance toward $T = 0$ above 4.0 T as in Fig. 1(a). They finally show a logarithmiclike increase down to 0.06 K above 6.7 T as in Fig. 1(b). In this Letter, we regard this weak divergence as a character of an "insulator" [9,14]. A strongly insulating behavior with exponential divergence is expected to appear by further decreasing temperature, even though the crossover temperature is inaccessibly low in general [7,40]. Strictly speaking, the state with the weak divergence is also classified as a dirty metal caused by quantum correction [7].

The existence of the zero-resistance phase, where pinned vortices form the vortex-glass (VG) phase, is confirmed on the logarithmic scale of MR curves (see Supplemental Material [41]). Boundary fields $B_c(T)$ between the VG phase and the vortex-liquid (VL) phase are extracted and plotted as filled black circles in the B-T plane in Figs. 2(a) and 2(b). From the linear extrapolation of $B_c(T)$ to $T = 0$, we estimate the superconductor-metal (SM) transition field $B_{\rm SM} = 4.4$ T at $T = 0$.

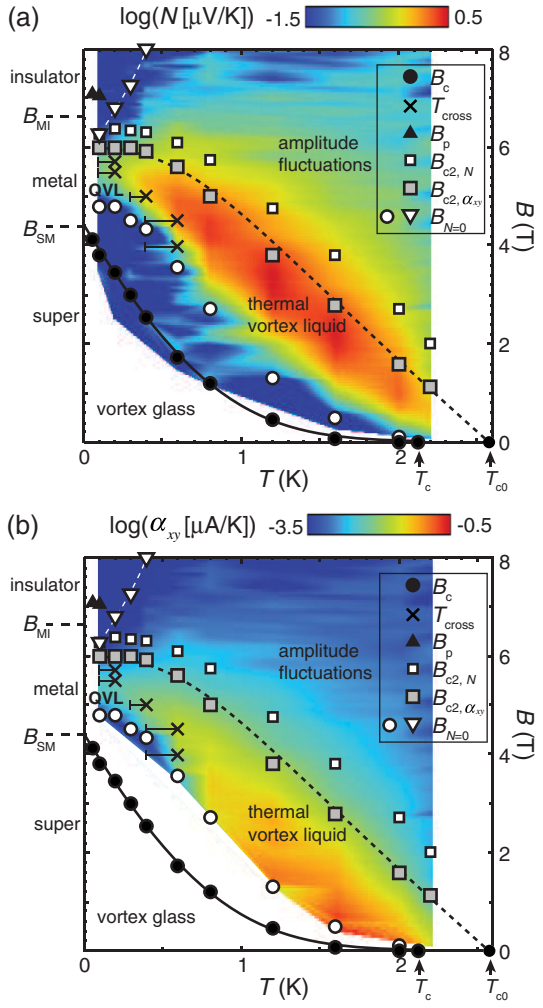

FIG. 2. Superconducting fluctuations revealed from Nernst effect measurements. Contour maps of N (a) and α_{xy} (b) are constructed from Figs. 3(a) and 3(c), respectively. Characteristic temperatures and fields are overplotted. Black circles, crosses, and black triangles denote B_c, $T_{\rm cross}$, and B_p, respectively, which are defined from $R_\square$. White circles, white squares, and white inverted triangles represent $B_{N=0,\rm low}$, $B_{c2,N}$ and $B_{N=0,\rm high}$, respectively, which are obtained from N. Gray squares show B_{c2} $(= B_{c2,\alpha_{xy}})$ determined from α_{xy}. A dashed white line, a dashed black line, and a solid black line along $B_{N=0,\rm high}$, B_{c2}, and B_c are guides to the eye, respectively.

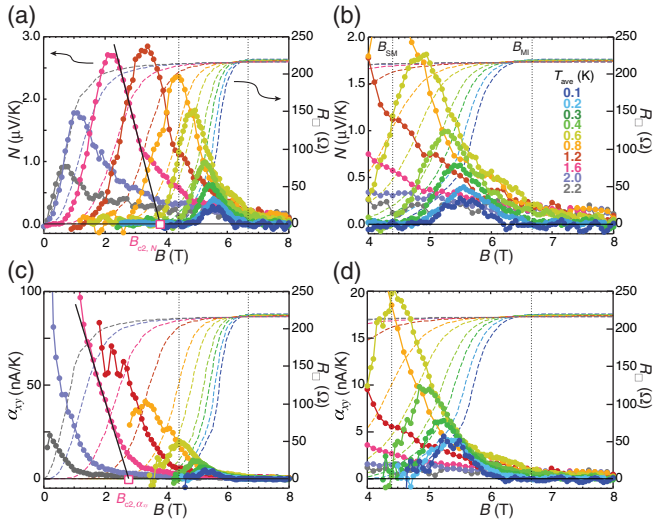

FIG. 3. Thermoelectric responses as a function of field. (a) Field dependence of N at fixed temperatures. MR curves are also displayed as dashed lines for comparison. Dotted lines show $B_{\rm SM}$ and $B_{\rm MI}$. A black straight line shows an example for a linear extrapolation of N to determine $B_{c2,N}$. (b) A high-field regime of (a) is enlarged. (c) Field dependence of α_{xy} converted from (a). A black straight line representatively shows the linear extrapolation of α_{xy} to determine $B_{c2}(= B_{c2,\alpha_{xy}})$. (d) A high-field regime of (c).

The metallic behavior is clearly seen in Arrhenius plots in Fig. 1(d). Deviation from a thermal activation formula $R_\square = R'_\square \exp(-U/k_B T)$, with which data in the high-temperature region are fitted as broken lines, becomes prominent above 4.0 T. Here, $R'_\square$ is a coefficient, U an activation energy for vortex motion, and k_B the Boltzmann constant. This is in sharp contrast to a-Mo_xSi_{1-x} without the deviation [46]. We roughly evaluate characteristic temperatures $T_{\rm cross}$, at which the deviation occurs, as denoted with arrows in Fig. 1(d) and plotted them in Figs. 2(a) and 2(b) as crosses. The flattened resistance below $T_{\rm cross}$ has been interpreted as a result of quantum tunneling of vortices [14]. Our main purpose is an experimental verification of this interpretation. We also extract U as in Fig. 1(e), which follows $U = U_0 \ln(B^*/B)$ [14,47] with $U_0/k_B = 4$ K and $B^* = 5.5$ T.

As shown in Fig. 1(b), a slope of the resistance in the low-temperature region changes its sign around 6.7 T, indicating a metal-insulator (MI) transition field $B_{\rm MI}$. The $B_{\rm MI}$ is confirmed in MR curves shown in Fig. 1(c) as a field at which the resistance becomes temperature independent at low temperatures.

Figures 3(a) and 3(b) display Nernst signals obtained by field sweep at fixed temperatures from 2.2 to 0.1 K. All of the data exhibit typical behavior of a vortex system 37–27]]. In the VG phase, Nernst signals are not observed. With increasing field, Nernst signals start to rise around B_c, and then decay after showing a peak. The growth of Nernst signals with increasing field is attributed to the reduced pinning effects for vortices due to thermal or quantum fluctuations and increase of vortex density in proportion to the field, which are mainly reflected in the field dependence of $R_\square$ in $N = R_\square \alpha_{xy}$. The subsequent decay originates from decrease of α_{xy}. Figures 3(c) and 3(d) show α_{xy} converted from N divided by $R_\square$. The vortex contribution to α_{xy} is represented by $\alpha_{xy}^\Phi = S_\Phi/\Phi_0$, where S_Φ is the transport entropy in the vortex core. S_Φ is proportional to $B_{c2} - B$ near the crossover field B_{c2} between the VL state and the normal state, and vanishes at B_{c2} [48,49]. Thus, we can roughly, but more clearly than resistance, estimate B_{c2} $(= B_{c2,\alpha_{xy}})$ from a linear extrapolation of α_{xy} to $\alpha_{xy} = 0$ as

shown with a solid black line in Fig. 3(c) [28,31,49]. This enables us to distinguish the contribution of the mobile vortices from that of amplitude fluctuations above B_{c2}. Extracted B_{c2}'s are plotted as gray squares in Figs. 2(a) and 2(b). These are linearly connected to $T_{c0} = 2.58$ K. Resistances at B_{c2} vary from 60% to 95% of the normal resistance from 2.2 to 0.1 K in order. We also plotted $B_{c2,N}$ in Figs. 2(a) and 2(b) as white squares, which are obtained by the linear extrapolation of N to $N = 0$ as shown with a solid black line in Fig. 3(a) [32,35]. The difference between $B_{c2,\alpha_{xy}}$ and $B_{c2,N}$ originates from large paraconductivity of $R_\square$ above B_{c2} $(= B_{c2,\alpha_{xy}})$ due to two dimensionality.

Figures 2(a) and 2(b) show contour maps of N and α_{xy}, respectively, along with characteristic fields and temperatures. Inside the VL phase defined by $B_c < B < B_{c2}$, the vortex Nernst signals are observed. We plot the low (high)-field limit $B_{N=0,\mathrm{low}}$ ($B_{N=0,\mathrm{high}}$), at which N becomes detectable in Figs. 3(a) and 3(b), as white circles (white inverted triangles) in Figs. 2(a) and 2(b). $B_{N=0,\mathrm{low}}$ is higher than B_c defined by resistance. This would come from a limited sensitivity of N to keep ΔT as low as possible or an intrinsic insensitivity of vortex motion to ΔT near the VG phase. It is noted that the vortex Nernst signals exist not only in the high-temperature region, but also near $T = 0$, indicating a direct signature of the mobile vortices due to quantum fluctuations. Therefore, we define this region as the quantum vortex-liquid (QVL) [50,51]. The field range of the QVL toward $T = 0$ remains nonzero inside the metallic state $B_{\mathrm{SM}} < B < B_{\mathrm{MI}}$. This result indicates that the anomalous metallic state originates from QVL, where the phase of SOP strongly fluctuates due to quantum fluctuations. As the origin of the dissipation at $T = 0$ in the metallic state, theories predict motion of dislocation-antidislocation pairs in VG generated by gauge-field fluctuations [23,24], bosonic excitations which fail to localize at $T = 0$ in superconducting puddles without the global phase coherence [25], and so on. Our finding cannot pick which model is right but experimentally verifies the existence of mobile vortices, which are essential in all the models [22–25].

Residual QVL toward $T = 0$ is confirmed in Fig. 4(a). The isomagnetic plots of N between 5.0 and 6.2 T decrease with decreasing temperature below 0.6 K and seem to reach $N = 0$ at $T = 0$, while those below 5.0 T fall to 0 at $T > 0$ near the VG phase. Observing the metallic behavior by the Nernst measurement as well as the resistance measurement strongly supports that it appears irrespective of external noise [52,53], because a dc or ac current source, the main possible origin of external noise, was removed from the sample in the Nernst measurement. N at 7.0 T represents the amplitude fluctuations ($B > B_{c2}$) in the insulating regime $B > B_{\mathrm{MI}}$. N in the insulating regime decreases with decreasing temperature and finally falls below the sensitivity as marked by $B_{N=0,\mathrm{high}}$ in Figs. 2(a) and 2(b). As highlighted by a dashed white line in Figs. 2(a) and 2(b),

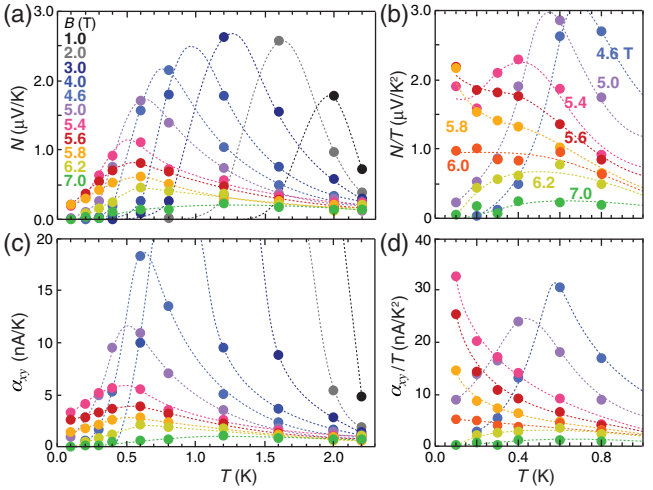

FIG. 4. Thermoelectric responses toward $T = 0$. Temperature dependences of N (a), N/T (b), α_{xy} (c), and α_{xy}/T (d) at fixed fields are extracted from Figs. 3(a) and 3(c). Dashed lines are guides to the eye.

$B_{N=0,\mathrm{high}}$ increases with increasing temperature. This trend is quite similar to a crossover line between the classical and the quantum fluctuations [37,54]. Although these theories predict a small negative N due to the quantum fluctuations just above the crossover field, it would be below the sensitivity in our measurement.

Figure 4(c) shows isomagnetic plots of α_{xy}, which unveil the striking thermodynamic feature of the metallic state. In contrast to the theory [48] and the previous experimental results for bulk superconductors [27,49], the decreasing behavior of α_{xy} toward $T = 0$ between 5.0 and 6.2 T is inconsistent with $S_\Phi \propto T$. As shown in Fig. 4(d), divergence of α_{xy}/T in the low temperature region highlights the deviation from $S_\Phi \propto T$. Similar divergent behaviors of ν/T [33] and C/T [55] have been known as the signs of the QCP of heavy-fermion systems, cuprates, etc. [3], where $\nu = N/B$ is a Nernst coefficient, and C specific heat. Significant increase of C toward the QCP is also reported in SIT [12]. Furthermore, the divergence of C/T in the anomalous metallic state was predicted in Ref. [23], where the authors state that the metallic state shows the character of a critical point. Therefore, we conclude that the unusual behavior of the transport entropy observed in the QVL strongly suggests the quantum criticality of the anomalous metallic state. Note that the critical character in the transport entropy is masked in the forms of N and N/T shown in Figs. 4(a) and 4(b), respectively, by a contribution of $R_\square$ to N.

To explain the origin of the emergence of the metallic state, the following scenario was plausibly proposed [26]. In the case of field-driven SIT, the metallic state is permitted only at the $T = 0$ QCP. At $T > 0$, a quantum critical regime is broadened into an area satisfying $\xi_{\mathrm{SI}}(B) > l_\phi(T)$, where $\xi_{\mathrm{SI}} \sim |B - B_{\mathrm{SI}}|^{-\nu}$ is a correlation

length of SIT, B_{SI} the QCP in SIT, ν a scaling exponent, $l_\phi \sim T^{-p}$ phase coherent length, and p an exponent for electron scattering. However, if divergence of l_ϕ at $T = 0$ is suppressed for some reason, e.g., coupling between a bosonic system and a fermionic background, the field range of the dissipative metallic state at $T = 0$ becomes nonzero from the criterion of $\xi_{SI}(B) > l_\phi(0)$. In other words, the metallic state originates from the broadening of QCP. The above scenario gives reasonable interpretation to our results in Figs. 4(c) and 4(d). As shown in Figs. 2(a) and 2(b), vanishing lines of N ($B_{N=0,\mathrm{low}}$ and $B_{N=0,\mathrm{high}}$) look like an expected boundary shape of the quantum critical regime. Thus, we suggest that the emergence of the anomalous metallic state is attributed to the broadened QCP in SIT.

Finally, we discuss the possibility of a Cooper-pair insulator in the insulator regime. Experimentally, the existence of the localized Cooper-pairs is indicated by a giant negative MR peak in the insulator phase, which often reaches several orders of magnitude larger than the normal resistance [6–10]. In this Letter, however, we observed only a slight hump in a MR curve at 0.06 K around $B_p \sim 7.0$ T in Fig. 1(c). Thus, the small negative MR would result from the amplitude fluctuations at extremely low temperatures rather than the localized Cooper pairs [7,56]. Moreover, we were not able to detect the vortex Nernst signals at $B \geq B_{MI}$. Since condensation of vortices is predicted in the Cooper-pair insulator [4,5], further investigations for more insulating films under high magnetic fields are quite interesting. At that time, it will be necessary to distinguish the contribution of vortices in a Nernst signal from that of the amplitude fluctuations.

We thank Ryusuke Ikeda for fruitful discussions. This work was supported by Grant-in-Aid for Young Scientists (KAKENHI Grants No. 17K14337 and No. 20K14413), Scientific Research B (KAKENHI Grant No. 17H02919) and Challenging Exploratory Research (KAKENHI Grant No. 15K13516) from the Japan Society for the Promotion of Science, and Grant for Research Seed and Ohsumi Research Grant for Fundamental Science from Tokyo Institute of Technology.

*ienaga.k.aa@m.titech.ac.jp
†okuma.s.aa@m.titech.ac.jp

[1] S. L. Sondhi, S. M. Girvin, J. P. Carini, and D. Shahar, Rev. Mod. Phys. **69**, 315 (1997).
[2] M. Vojta, Rep. Prog. Phys. **66**, 2069 (2003).
[3] H. v. Löhneysen, A. Rosch, M. Vojta, and P. Wölfle, Rev. Mod. Phys. **79**, 1015 (2007).
[4] M. P. A. Fisher, G. Grinstein, and S. M. Girvin, Phys. Rev. Lett. **64**, 587 (1990).
[5] M. P. A. Fisher, Phys. Rev. Lett. **65**, 923 (1990).
[6] A. M. Goldman and N. Marković, Phys. Today **51**, No. 11, 39 (1998).
[7] V. F. Gantmakher and V. T. Dolgopolov, Phys. Usp. **53**, 1 (2010).
[8] M. A. Paalanen, A. F. Hebard, and R. R. Ruel, Phys. Rev. Lett. **69**, 1604 (1992).
[9] S. Okuma, T. Terashima, and N. Kokubo, Phys. Rev. B **58**, 2816 (1998).
[10] G. Sambandamurthy, L. W. Engel, A. Johansson, and D. Shahar, Phys. Rev. Lett. **92**, 107005 (2004).
[11] A. Roy, E. Shimshoni, and A. Frydman, Phys. Rev. Lett. **121**, 047003 (2018).
[12] S. Poran, T. Nguyen-Duc, A. Auerbach, N. Dupuis, A. Frydman, and O. Bourgeois, Nat. Commun. **8**, 14464 (2017).
[13] A. Kapitulnik, S. A. Kivelson, and B. Spivak, Rev. Mod. Phys. **91**, 011002 (2019).
[14] D. Ephron, A. Yazdani, A. Kapitulnik, and M. R. Beasley, Phys. Rev. Lett. **76**, 1529 (1996).
[15] Y. Qin, C. L. Vicente, and J. Yoon, Phys. Rev. B **73**, 100505 (R) (2006).
[16] N. P. Breznay and A. Kapitulnik, Sci. Adv. **3**, e1700612 (2017).
[17] Z. Han, A. Allain, H. Arjmandi-Tash, K. Tikhonov, M. Feigel'man, B. Sacépé, and V. Bouchiat, Nat. Phys. **10**, 380 (2014).
[18] Y. Saito, Y. Kasahara, J. Ye, Y. Iwasa, and T. Nojima, Science **350**, 409 (2015).
[19] A. W. Tsen, B. Hunt, Y. D. Kim, Z. J. Yuan, S. Jia, R. J. Cava, J. Hone, P. Kim, C. R. Dean, and A. N. Pasupathy, Nat. Phys. **12**, 208 (2016).
[20] S. Ichinokura, Y. Nakata, K. Sugawara, Y. Endo, A. Takayama, T. Takahashi, and S. Hasegawa, Phys. Rev. B **99**, 220501(R) (2019).
[21] A. Benyamini, E. J. Telford, D. M. Kennes, D. Wang, A. Williams, K. Watanabe, T. Taniguchi, D. Shahar, J. Hone, C. R. Dean, A. J. Millis, and A. N. Pasupathy, Nat. Phys. **15**, 947 (2019).
[22] E. Shimshoni, A. Auerbach, and A. Kapitulnik, Phys. Rev. Lett. **80**, 3352 (1998).
[23] D. Das and S. Doniach, Phys. Rev. B **60**, 1261 (1999).
[24] D. Das and S. Doniach, Phys. Rev. B **64**, 134511 (2001).
[25] D. Dalidovich and P. Phillips, Phys. Rev. Lett. **89**, 027001 (2002).
[26] A. Kapitulnik, N. Mason, S. A. Kivelson, and S. Chakravarty, Phys. Rev. B **63**, 125322 (2001).
[27] P. R. Solomon and F. A. Otter, Jr., Phys. Rev. **164**, 608 (1967).
[28] H.-C. Ri, R. Gross, F. Gollnik, A. Beck, R. P. Huebener, P. Wagner, and H. Adrian, Phys. Rev. B **50**, 3312 (1994).
[29] R. Ikeda, Phys. Rev. B **66**, 100511(R) (2002).
[30] Y. Wang, Z. A. Xu, T. Kakeshita, S. Uchida, S. Ono, Y. Ando, and N. P. Ong, Phys. Rev. B **64**, 224519 (2001).
[31] Y. Wang, N. P. Ong, Z. A. Xu, T. Kakeshita, S. Uchida, D. A. Bonn, R. Liang, and W. N. Hardy, Phys. Rev. Lett. **88**, 257003 (2002).
[32] Y. Wang, L. Li, and N. P. Ong, Phys. Rev. B **73**, 024510 (2006).
[33] K. Izawa, K. Behnia, Y. Matsuda, H. Shishido, R. Settai, Y. Onuki, and J. Flouquet, Phys. Rev. Lett. **99**, 147005 (2007).

[34] A. Pourret, H. Aubin, J. Lesueur, C. A. Marrache-Kikuchi, L. Bergé, L. Dumoulin, and K. Behnia, Nat. Phys. **2**, 683 (2006).
[35] A. Pourret, H. Aubin, J. Lesueur, C. A. Marrache-Kikuchi, L. Bergé, L. Dumoulin, and K. Behnia, Phys. Rev. B **76**, 214504 (2007).
[36] I. Ussishkin, S. L. Sondhi, and D. A. Huse, Phys. Rev. Lett. **89**, 287001 (2002).
[37] M. N. Serbyn, M. A. Skvortsov, A. A. Varlamov, and V. Galitski, Phys. Rev. Lett. **102**, 067001 (2009).
[38] S. Okuma, K. Kashiro, Y. Suzuki, and N. Kokubo, Phys. Rev. B **77**, 212505 (2008).
[39] K. Ienaga, T. Arai, T. Hayashi, S. Kaneko, and S. Okuma, J. Phys. Conf. Ser. **1293**, 012022 (2019).
[40] Y. Liu, D. B. Haviland, B. Nease, and A. M. Goldman, Phys. Rev. B **47**, 5931 (1993).
[41] See Supplemental Material at http://link.aps.org/supplemental/10.1103/PhysRevLett.125.257001 for an analysis determining the vortex-glass state, which includes Refs. [42–45].
[42] T. Klein, A. Conde-Gallardo, J. Marcus, C. Escribe-Filippini, P. Samuely, P. Szabó, and A. G. M. Jansen, Phys. Rev. B **58**, 12411 (1998).
[43] N. Mason and A. Kapitulnik, Phys. Rev. B **64**, 060504(R) (2001).
[44] D. S. Fisher, M. P. A. Fisher, and D. A. Huse, Phys. Rev. B **43**, 130 (1991).
[45] H. Sato and S. Okuma, J. Phys. Conf. Ser. **400**, 022103 (2012).
[46] S. Okuma, T. Kishimoto, and K. Kainuma, Physica (Amsterdam) **437C–438C**, 247 (2006).
[47] M. V. Feigel'man, V. B. Geshkenbein, and A. I. Larkin, Physica (Amsterdam) **167C**, 177 (1990).
[48] K. Maki, Phys. Rev. Lett. **21**, 1755 (1968).
[49] F. Vidal, Phys. Rev. B **8**, 1982 (1973).
[50] S. Okuma, S. Togo, and M. Morita, Phys. Rev. Lett. **91**, 067001 (2003).
[51] T. Sasaki, T. Fukuda, T. Nishizaki, T. Fujita, N. Yoneyama, N. Kobayashi, and W. Biberacher, Phys. Rev. B **66**, 224513 (2002).
[52] I. Tamir, A. Benyamini, E. J. Telford, F. Gorniaczyk, A. Doron, T. Levinson, D. Wang, F. Gay, B. Sacépé, J. Hone, K. Watanabe, T. Taniguchi, C. R. Dean, A. N. Pasupathy, and D. Shahar, Sci. Adv. **5**, eaau3826 (2019).
[53] S. Dutta, I. Roy, S. Mandal, J. Jesudasan, V. Bagwe, and P. Raychaudhuri, Phys. Rev. B **100**, 214518 (2019).
[54] A. Glatz, A. Pourret, and A. A. Varlamov, arXiv:2007.15865 [Phys. Rev. X (to be published)].
[55] Y. Matsumoto, S. Nakatsuji, K. Kuga, Y. Karaki, N. Horie, Y. Shimura, T. Sakakibara, A. H. Nevidomskyy, and P. Coleman, Science **331**, 316 (2011).
[56] V. M. Galitski and A. I. Larkin, Phys. Rev. B **63**, 174506 (2001).